Radiation-hydrodynamic simulations of backlighter options for FAIR

S. Faik [(1)], M.M. Basko [(2,3)], J. Jacoby [(1)], T. Manegold [(1)], O. Rosmej [(1,3)], An. Tauschwitz [(1)]

[(1)] Goethe University, Frankfurt, Germany, [(2)] KIAM, Moscow, Russia, [(3)] GSI, Darmstadt, Germany

GOETHE UNIVERSITÄT FRANKFURT AM MAIN

GEFÖRDERT VOM Bundesministerium für Bildung und Forschung

Planned plasma physics experiments at the upcoming FAIR accelerator facility providing a new unique environment to study warm and hot dense matter states demand for new diagnostic techniques. Such diagnostics include VUV- and X-ray backlighter sources. Correct modeling of the evolution and power deposition in such targets is a computationally and numerically challenging task. The two-dimensional hydrodynamics code RALEF-2D [1] with multigroup radiation transport and thermal conduction allows for simulations of laser-heated target configurations and matter at High Energy Density. A newly developped laser package includes laser-light refraction and reflections as well as power deposition in the overcritical plasma regime.

RALEF-2D

Mesh: two-dimensional, quadrilateral cells, multi-block, cartesian (x, y) or axisymmetric (r, z) coordinates

Hydrodynamics: local, based on the code CAVEAT [2], Arbitray-Lagrangian-Eulerian (ALE) remapping, Godunov-like Riemann solver, 2nd order in space

Thermal conduction: local, symmetrical-semi-implicit (SSI) method [3], 2nd order in space

Radiation transport: non-local, angular discretization with the S_n-method [4], SSI, short characteristics, 2nd order in space, discrete spectral groups $[\nu_j, \nu_{j+1}]$ with Planckian averaged absorption coefficient k_ν

Laser absorption: old model without refraction and deposition by inverse bremsstrahlung; new model with refraction [5], see below

Supercomputing: parallelization with MPI / OpenMP

EOS and opacity models

THERMOS code (KIAM, Moscow): provides EOS, thermal conductivity and spectral opacities [6]; spectral opacities are generated from the Hartree-Fock-Slater equation for plasma ions with equilibrium level population (LTE)

FEOS package (Geothe University): provides EOS for any chemical element and arbitrary mixtures; Thomas-Fermi model and ionic model by Cowan; Maxwell construction for realistic EOS for simulations within liquid-vapor two-phase region [7]; library-based code design and visualization tool

Advanced laser simulation algorithm

Requirements: calculation of the refracted laser light distribution and of the deposited and reflected powers and the angular distribution of the reflected laser light close to and above the critical free electron density $(n_e \gtrsim n_c)$

Applied solution: spatially discretize the incoming laser beam intensity, apply 2D geometrical optics approach with refraction for undercritical free electron densities $(n_e \ll n_c)$, and augment it by a 1D wave optics solver for complex refractive indices σ $(n_e \gtrsim n_c)$

Computational implementation: split rays at critical surfaces into straight wave optics rays propagating parallel to the density gradient of the entry cell $(n_e \gtrsim n_c)$ and reflected geometrical optics rays

2D geometrical optics:

On the basis of the eikonal equation [8] the equation of motion of a ray [9] for $n_e \ll n_c$ becomes:

$$d^2\vec{r}/dt^2 = -(c^2/2)(\vec{\nabla} n_e/n_c) \quad (1)$$

Deposited power on ray segment Δs in crossed cell:

$$P_{dep} = P_0\left(1 - e^{-\kappa}\right), \quad \kappa = \Delta s \, \mathrm{Im}\,(\sigma) \quad (2)$$

P_0 – initial power, κ – optical depth, σ – complex refractive index of cell (per unit length, inverse bremsstrahlung)

1D wave optics solver:

Crossed cell segments define a piecewise-constant distribution of permittivities ϵ_j along the ray coordinate z

Solve Maxwells equations and calculate deposited, reflected, and transmitted ray energies from the field components $\vec{F}_j^s = (E_{x,j}, H_{y,j})$ for s- or $\vec{F}_j^p = (H_{x,j}, -E_{y,j})$ for p-polarization with the amplitudes $\vec{A}_j = \left(A_j^+, A_j^-\right)$ of the superposition of the incident and reflected waves

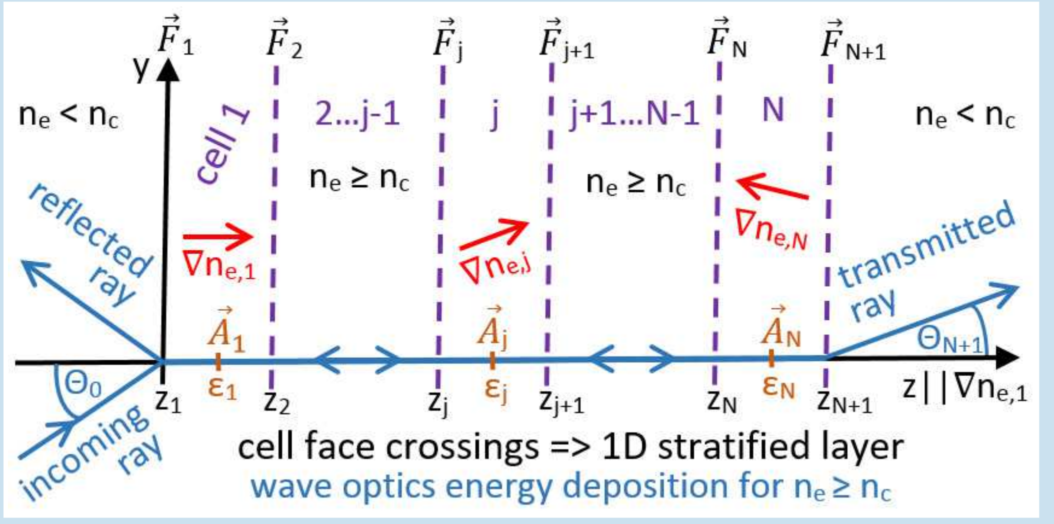

Figure 1: 1D wave optics solver for a stratified medium [8]

Simulations of hohlraum targets

Example: heating of a carbon foam by hohlraum X-rays for energy loss measurements of heavy ions in partially ionized plasmas using the PHELIX laser and the Unilac at GSI [10]

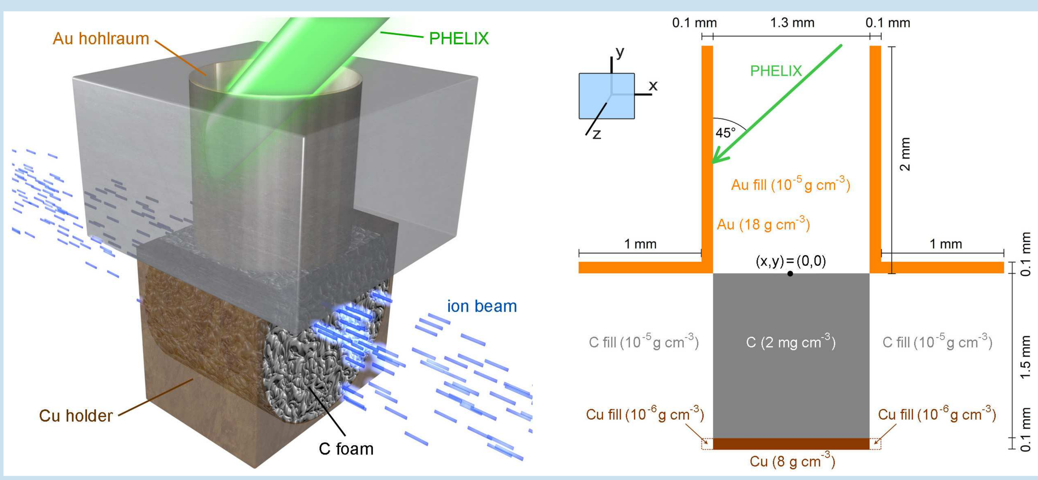

Figure 2: (left) Schematic view of the target geometry; (right) Simulation setup with dimensions and initial densities

PHELIX laser: $\lambda_l = 527$ nm, $E = 180$ J, $t_{pulse} = 1.4$ ns

Simulation on an ALE-mesh with ≈ 110000 cells

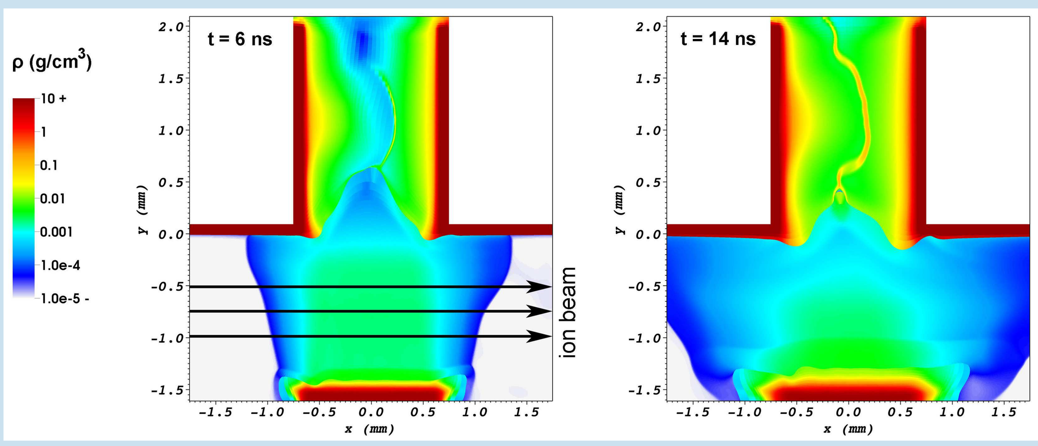

Figure 3: Color contour plot of the simulated matter density ρ of the whole experimental configuration at $t = 6$ and 14 ns

Laser reflections to include in future simulations

Plasma gun backlighter

Ion-beam heated foils require an intense VUV-backlighter $(10 - 15$ eV). At Goethe University a helium plasma can be accelerated by a plasma gun and compressed inside conically shaped glas targets providing such a VUV source.

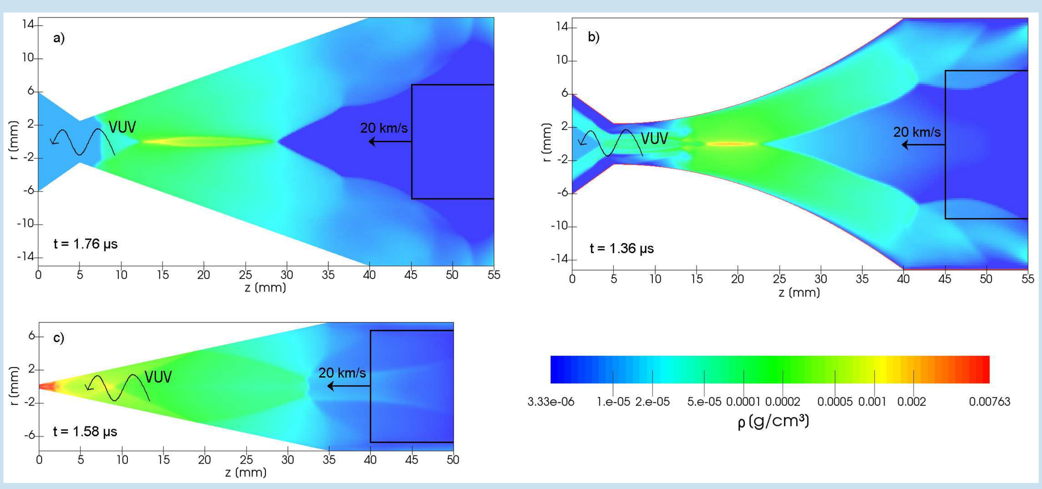

Figure 4: Simulations of matter density of a helium plasma shot by plasma gun and compressed in a) open cone, b) open trumpet, and c) closed cone glass targets

Simulations have been performed to find the best geometry for maximum compression and heating. Fig. 4 shows three simulated configurations initially filled with helium gas at room temperature and 60 mbar pressure and an initial velocity of 20 km/s of the already 10-times compressed plasma cloud at the exit of the plasma gun.

Further spectral measurements and simulations including the radiation transport are planned.

Hohlraum backlighter

For mid-Z plasmas like μm-thin carbon foils which will be used at FAIR an intense smooth backlighter option is needed where the spectrum should not be tainted with dominating spectral lines. Fig. 5 shows a simulation of a gold hohlraum backlighter target with length 0.8 mm and diameter 0.8 mm heated by the short pulse $(10$ ps, 50 J) option of the PHELIX laser at GSI with a peak maximum of the simulated hohlraum spectra at $100 - 120$ eV.

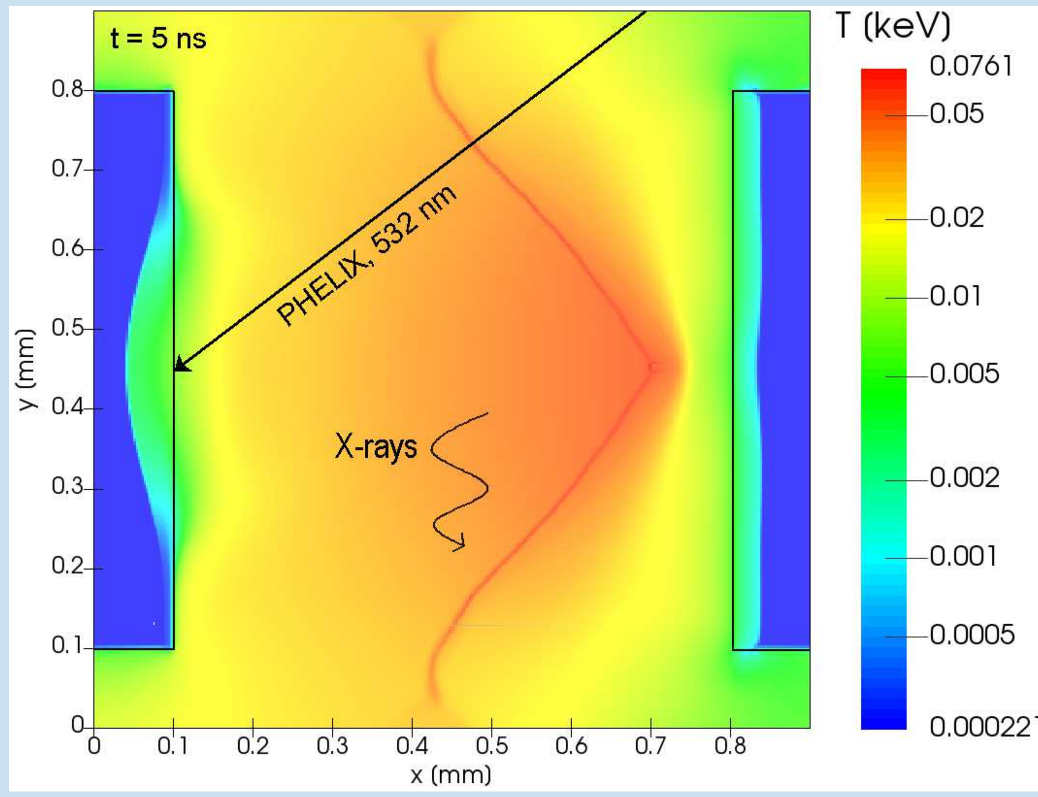

Figure 5: Simulated temperature inside a 0.8 mm long gold hohlraum with diameter 0.8 mm at $t = 5$ ns. The hohlraum is heated by the short pulse of the PHELIX laser. Black lines indicate the boundary of the hohlraum walls and the direction and spot of the laser at $t = 0$ ns. Plasma is ablated from the left hohlraum wall by the laser beam and from the right wall by thermal radiation. Both plasma fronts collide and form a hot filament close to the hohlraum center.

Fig. 6 shows the calculated X-ray spectrum as would have been observed through the lower hohlraum hole at three times and in comparison to a Planckian fit for $T = 33$ eV. At $t = 5$ ns the spectrum comes close to the Planckian one with a peak maximum of the spectrum at $100 - 120$ eV. At $t = 20$ ns, both the matter and radiation temperature close to the hohlraum center drop down only by 15% compared to the temperatures at $t = 5$ ns. This shows that the hohlraum can be used over a long time period with $T \approx 28 - 33$ eV for backlighting.

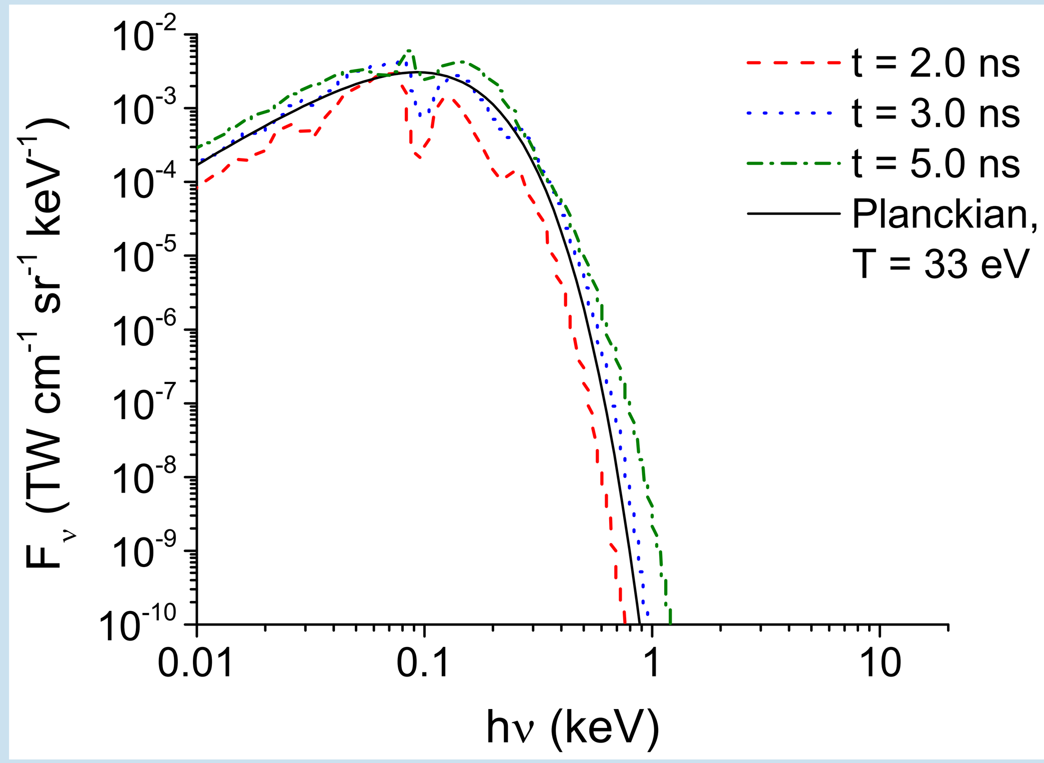

Figure 6: Calculated X-ray spectrum as would have been observed through the lower hohlraum hole at $t = 2$, 3, and 5 ns. The solid line shows a Planckian fit for $T = 33$ eV.

Acknowledgments

This work is supported by BMBF project No. 05P15RGFAA.

[1] M.M. Basko, An. Tauschwitz, J. Maruhn; GSI Report 2010-1 (GSI Scientific Report 2009), p. 410; [2] F.L. Addessio, J.R. Baumgardner, J.K. Dukowicz, N.L. Johnson, B.A. Kashiwa, R.M. Rauenzahn, C. Zemach; LANL, LA-10613-MS, Rev. 1 (1992); [3] E. Livne, A. Glasner; J. Comp. Physics **58** (1985) 59; [4] B.G. Carlson; in Methods in Computational Physics, p. 1, Academic Press, New York and London (1963);
[5] M.M. Basko, I.P. Tsygvintsev; Computer Physics Communications (2017) 6128; [6] A.F. Nikiforov, V.G. Novikov, V.B. Uvarov; "Quantum-Statistical Models of Hot Dense Matter"; Birkhäuser (2005); [7] S. Faik, M.M. Basko, An. Tauschwitz, I. Iosilevskiy, J.A. Maruhn; High Energy Density Physics 8 (2012) 349; [8] M. Born, E. Wolf; "Principles of Optics"; Cambridge University Press (2005); [9] T.B. Kaiser; Physical Review E 61 (2000) 895;
[10] S. Faik, An. Tauschwitz, M.M. Basko, J.A. Maruhn, O. Rosmej, T. Rienecker, V.G. Novikov, A.S. Grushin; High Energy Density Physics 10 (2014) 1574.

DIN A4 lesbares Literaturverzeichnis

References

[1] M.M. Basko, An. Tauschwitz, J. Maruhn; GSI Report 2010-1 (GSI Scientific Report 2009), p. 410;

[2] F.L. Addessio, J.R. Baumgardner, J.K. Dukowicz, N.L. Johnson, B.A. Kashiwa, R.M. Rauenzahn, C. Zemach; LANL, LA-10613-MS, Rev. 1 (1992);

[3] E. Livne, A. Glasner; J. Comp. Physics **58** (1985) 59;

[4] B.G. Carlson; in Methods in Computational Physics, p. 1, Academic Press, New York and London (1963);

[5] M.M. Basko, I.P. Tsygvintsev; Computer Physics Communications (2017) 6128;

[6] A.F. Nikiforov, V.G. Novikov, V.B. Uvarov; "Quantum-Statistical Models of Hot Dense Matter"; Birkhäuser (2005);

[7] S. Faik, M.M. Basko, An. Tauschwitz, I. Iosilevskiy, J.A. Maruhn; High Energy Density Physics 8 (2012) 349;

[8] M. Born, E. Wolf; "Principles of Optics"; Cambridge University Press (2005);

[9] T.B. Kaiser; Physical Review E 61 (2000) 895;

[10] S. Faik, An. Tauschwitz, M.M. Basko, J.A. Maruhn, O. Rosmej, T. Rienecker, V.G. Novikov, A.S. Grushin; High Energy Density Physics 10 (2014) 1574;